Phosphate-Free Inhibition of Calcium Carbonate Dishwasher Deposits

Yuexian Hong,[a] Nathalie Letzelter,[b] John S. O. Evans,[a] Dmitry S. Yufit,[a] Jonathan W. Steed[a]*

(a) Department of Chemistry, Durham University, South Road, Durham, DH1 3LE, United Kingdom. Email: jon.steed@durham.ac.uk

(b) Procter & Gamble Newcastle Innovation Centre, Longbenton, Whitley Road, Newcastle upon Tyne, NE12 9BZ, United Kingdom

Abstract

This paper reports the characterization of the composition and morphology of mineral formation on glass and plastic (polymethylmethacrylate) substrates in a dishwasher environment and the identification of suitable phosphate-free mineral crystallization inhibitors as environmentally benign candidates to replace the currently used phosphate-containing inhibitor 1-hydroxyethane 1,1-diphosphonic acid (HEDP). Screening of the calcium carbonate crystallization inhibition performance of twenty-eight different compounds resulted in the identification of two phosphate-free, cyclic polycarboxylic acid inhibitors, which were found in combination to be effective replacements. Each inhibitor proved to be highly substrate specific with all-*cis*-cyclohexane-1,2,3,4,5,6-hexacarboxylic acid (CHHCA) preventing deposition on glass (where calcite is the dominant polymorph) and *cis,cis,cis,cis*-cyclopentane-1,2,3,4-tetracarboxylic acid (CPTCA) inhibiting aragonite deposition on polymethylmethacrylate (PMMA). When used in combination,

these two species prevented all forms of calcium carbonate deposition on both substrate types. The underlying inhibition mechanism and structural requirements of an efficient calcium carbonate inhibitor are also discussed.

Introduction

Deposition of calcium carbonate in dishwashers, particularly on plastic, remains a problem. Conditions inside dishwashers such as water hardness, high temperature, high pH and high ionic strength all promote the precipitation of calcium carbonate. Currently, chemical and non-chemical treatments have been applied to prevent surface deposition[1-2] and yet only ion exchange softening, acid dosing and the use of the antiscalants are capable of achieving effective scale control.[3] The use of antiscalants still seems the easiest way to achieve scale control because ion exchange softening relies upon expensive semipermeable membranes, while acid dosing can cause serious corrosion issues.[1]
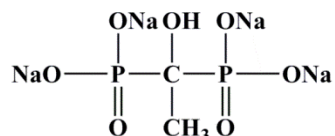

Figure 1. Structure of 1-hydroxyethane 1, 1-diphosphonic acid (HEDP) as its tetrasodium salt.

In dishwasher detergents, the antiscalant is called the 'inhibitor.' The most common inhibitors currently used in dishwasher detergents are phosphonate salts. They are used to prevent the formation of inorganic deposits, particularly calcium carbonate.[4] However, due to their environmental impact, the usage of phosphate-containing inhibitors are banned in some States of the USA and further regulations elsewhere in the world seems likely. Therefore, new phosphate-free inhibitors are needed to replace the commonly used tetrasodium salt of 1-hydroxyethane 1,1-diphosphonic acid (HEDP, Figure 1).

So far, six different crystal forms of calcium carbonate with decreasing stabilities have been observed, namely, calcite, aragonite, vaterite, calcium carbonate monohydrate, calcium carbonate hexahydrate and amorphous calcium carbonate.[5] Calcite and aragonite are the most thermodynamically stable structures and are observed extensively in biomineralization[5] and in an industrial context.[6-9] Calcite is the most thermodynamically stable form at room temperature, while aragonite, which is about 1.5 times as soluble as calcite, is favored by crystallization at higher temperature and pressure.[10] Most inhibition performance assessment has been carried out by a constant composition method[11] based on the ability of an inhibitor to reduce the rate of crystal growth on seeded calcite[12-15] or seeded aragonite.[16] The mode of action of the inhibitor before the formation of the seeded crystals has been largely ignored. Whether a given inhibitor affects the nucleation stage rather than crystal growth[17, 18] or both[2, 19] or just simply inhibits the aggregation of the primary particles[20] is still under investigation, partly because the molecular-level processes of the nucleation stage involved are currently inaccessible to experiment.[21] HEDP has been widely studied as an efficient inhibitor for seeded calcite[22-23] and seeded aragonite.[24] Its inhibition capability as a nucleation inhibitor has been discussed for hydroxyapatite formation, showing that the use of 50 μM HEDP is able to delay the transformation of amorphous calcium phosphate to hydroxyapatite for 40 minutes.[25] However, whether HEDP acts with calcium carbonate before nucleation or during crystal growth or both is still unknown.

Based on an understanding of the structure nature of HEDP[26-27] and the suggestion by Anwar,[21] it is likely that an effective inhibitor should consist of strong calcium-binding functional groups linked by a two to five carbon atom spacer in the aliphatic chain[11, 28] with the ability to disrupt the periodicity of the emerging crystal nucleus. This inhibitor should be solute-

philic rather than amphiphilic (with an affinity for both solute and solvent) and have a low degree of self-association.[21] Both aromatic oligo-carboxylates and cyclic oligo-carboxylates, with two or more carboxylate groups attached to different carbon atoms in the ring (with a similar spacer as comparable to linear oligo-carboxylates), appear to satisfy these requirements and potentially represent an environmentally benign replacement for HEDP.[12-14]
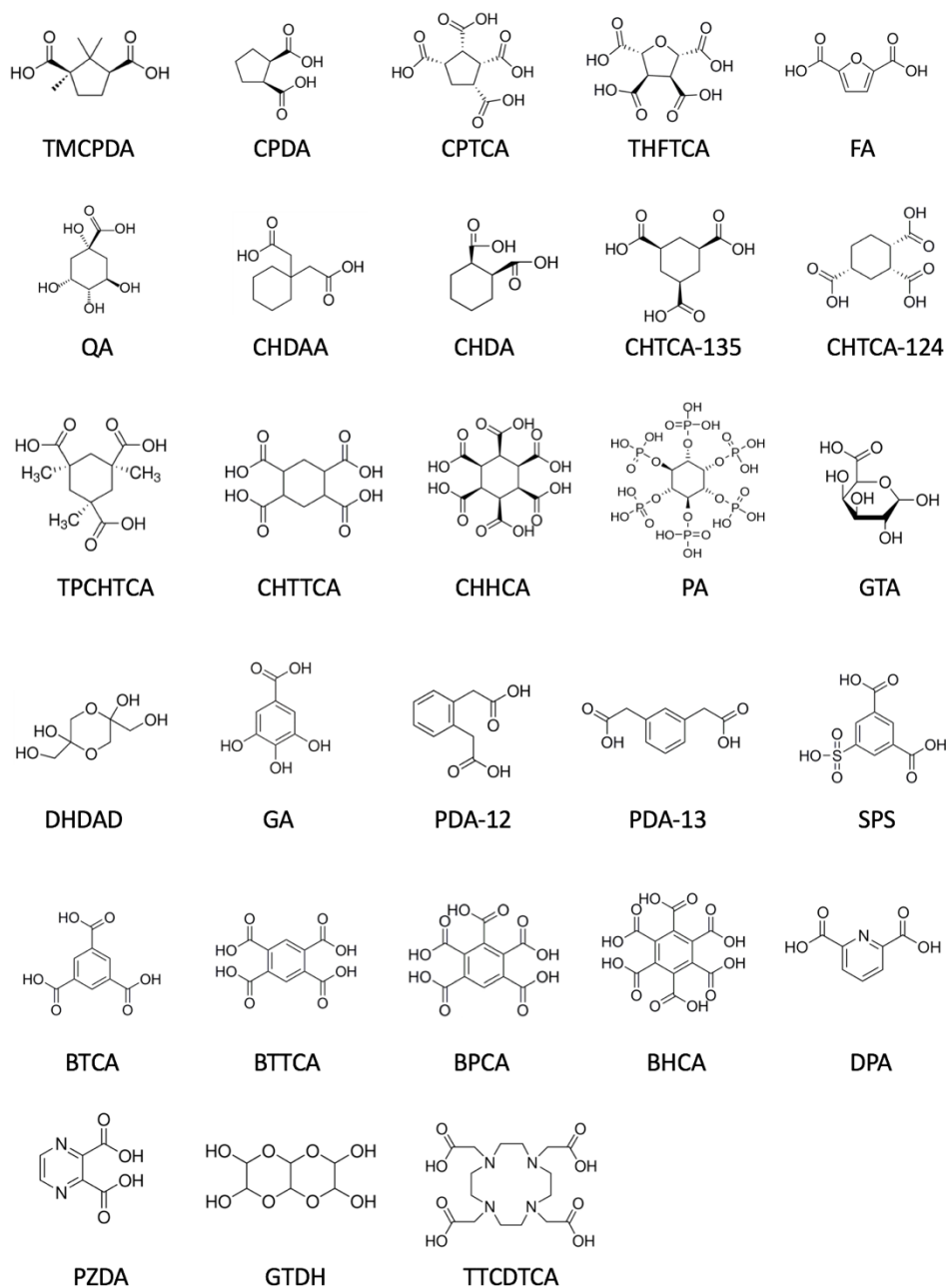

TMCPDA　　CPDA　　CPTCA　　THFTCA　　FA

QA　　CHDAA　　CHDA　　CHTCA-135　　CHTCA-124

TPCHTCA　　CHTTCA　　CHHCA　　PA　　GTA

DHDAD　　GA　　PDA-12　　PDA-13　　SPS

BTCA　　BTTCA　　BPCA　　BHCA　　DPA

PZDA　　GTDH　　TTCDTCA

Figure 2. Structures of the selected candidate inhibitors.

It has been shown that the linear polycarboxylic acids have little or no inhibition ability for calcite,[12] while cyclic oligo-carboxylates, especially those with four or more carboxylate groups can be effective inhibitors for seeded calcite.[12-13] This is consistent with results obtained for benzoic acids. Richmond[14] examined benzoic acids with two to six carboxylic acid groups and showed that the more carboxylate groups attached to the benzene-derived ring, the better the inhibition outcome for seeded calcite. Benzene-1,2,3,4,5,6-hexacarboxylic acid proved to have the best inhibition performance for seeded calcite, followed by isophthalic acid (benzene-1,3-dicarboxylic acid), indicating that two carboxylic acids situated on an aromatic ring can also cause inhibition effects. These inhibitors are commonly used in the context of crystal growth inhibition of seeded calcite in solution. However, inhibitors for seeded crystals may not be effective nucleation inhibitors.[21, 29] Moreover, calcite may be not the only polymorph of calcium carbonate observed in the dishwasher system. One inhibitor that is effective for one polymorph may not be effective for all possible solid forms. Therefore, under a given set of conditions, each inhibitor needs to be tested before application.[30]

Cyclic polycarboxylic acids have not been systematically studied in an inhibition context in the rather special conditions within the dishwasher environment. In this work, we examine the calcium carbonate crystallization inhibition efficiency of twenty-eight different commercially available cyclic di- and oligocarboxylate inhibitors of the type shown in Figure 2. Some inhibitors examined in this work include compounds that have been suggested as effective inhibitors for seeded aragonite[16] and seeded calcite[12-13, 15] The inhibition performance and polymorphic and substrate specificity were compared to the currently used HEDP standard.

Experimental Section

A Model Dishwasher System

A model dishwasher system was developed to allow rapid laboratory screening of candidate inhibitors. In the model set-up, substrates were fixed near the top of the glass container. A hot plate with a thermometer was used to maintain the temperature at 65 °C. Stirring at 100 rpm was used to disperse the detergent without causing significant agitation effects. PMMA sheets and glass sheets were fixed in pairs near the top of the container. Hard water was prepared by dissolving $CaCl_2$ (0.1526 g, 2.75 mmol L^{-1}) and $MgCl_2$ (0.0408 g, 0.86 mmol L^{-1}) in 500 mL deionized water (DI water). This solution was then transferred into the container and heated to 65 °C, before the addition of the dishwasher formula. The formula composition of the dishwasher detergent is listed in Table 1. For experiments without HEDP, the same formula was used without the HEDP additive ('nil-HEDP formula').

Table 1. Prototype dishwasher detergent (HEDP formula).

Prototype formula	Abbreviation	Quantity (g) in 0.5 L	Comments
Alkaline builder			
Trisodium salt of methylglycinediacetic acid	MGDA	0.282	Chelator
Granular sodium carbonate	Na_2CO_3	0.954	pH buffer
Sodium sulfate	Na_2SO_4	0.306	Solid diluter
Polymer			
Sulfonated polyacrylates Acusol 588	Acusol 588G	0.129	
Surfactant			
Non-ionic mixture	Non-ionic mixture	0.128	SLF180 & TO7 (BASF)
Inhibitor			
1-hydroxyethane 1,1-diphosphonic acid	HEDP	0.016	

In the model system, the amount of water and the amount of the formula is ten times less than that used in the dishwasher itself (Table S1, Supporting Information). To make all the detergent compositions dissolve at a similar speed, all powdered compositions were added simultaneously except the liquid non-ionic surfactant mixture, which was added last due to its high dissolution speed. Detergent was dispersed and contributed to an average pH value of 10.5 in the solution. The container then was covered, and the solution kept at 65 °C for 60 min. After 60 min, the PMMA sheets and glass sheets were taken out, rinsed first with cold DI water and then again with DI water at 60 °C for one minute each. The substrates were left in the air to dry. Two sheets of each substrate were retained each time for analysis, and the remainder replaced in fresh hard water and detergent solution and the procedure repeated. Details of the chemicals in Table 1 is given in Table S2 of the Supporting Information.

Characterization

Characterization of Solid Deposits

The clarity of samples produced in a commercial dishwasher was graded by a camera analysis rating system in which pictures of transparent substrates were taken against a black background in an environment with controlled lighting. The mean film gray level is a measurement of gray level in the range 0-255 and the clarity (%) is calculated by normalizing the gray scale to 100%. Thus, a clarity index of 100 would occur with a completely dark (transparent) glass and with a gray level of zero indicating no film present. In the model system, the clarity of samples was rated *via* naked eye evaluation as the sheets from the model system were too small to be evaluated in the camera analysis system. No correlation between the scores of the visual grading and imaging system was attempted.

Powder X-ray diffraction (PXRD) patterns were collected on a Bruker D8 powder diffractometer using a nickel- filtered $K\alpha_{1/2}$ copper X-ray radiation operating at 40 mA and 45 kV. The 2θ range for data collection for surface calcium carbonate and the synthesized calcium coordination complexes (CPTCA-Ca, *vide infra*) was 15°– 70° and 2°– 60°, respectively, at a scan rate of 0.02 step^{-1}. The data were analyzed by using Rietveld refinement performed with Topas Academic software.[31] Two PXRD patterns were collected for each sample, one *in situ* with the unbroken deposits on the substrate and one on free material scraped from the substrate surface. The PXRD outcome shown in the following tables combines analysis of the two patterns. The PXRD pattern collected with substrate is often affected by the preferred orientation of the crystalline material and the powder scraped from the substrate gives better information on the polymorph distribution ratio. Attenuated total reflection infrared spectroscopy (AIR-IR) was also applied for deposits identification. The IR spectra were recorded on a Perkin Elmer Spectrum 100 using a diamond compression cell and collected in the 4000–400 cm^{-1} region at a resolution of 4 cm^{-1}. Typically, 32 scans were conducted for a spectrum. The resulting IR spectra were analyzed with the software KnowItAll.[32]

The morphology of the resulting deposits was imaged by scanning electron microscopy (SEM). The samples were coated with gold/palladium prior to imaging in a HITACHI S-520 type SEM combined with an energy-dispersive X-ray spectroscopy (EDX).[33] In EDX mode, a voltage of 10 kV was applied. Typically, a field free mode, operated at a voltage of 5 kV to 8 kV, was used for sample imaging. Transmission electron microscopy (TEM) combined with EDX was mainly used for the identification of a specific morphology for calcium carbonate or to confirm the preferred orientation of one specific polymorph. Samples for TEM were prepared by scraping the material from filmed surfaces of substrates, dispersing them in acetone, and dropping this

suspension over a holey copper grid. Electron diffraction was carried out on a JEOL 2100F FEG TEM in transmission mode operating at 200 eV. EDX data for the samples were collected at the same time. The control of the process and the diffraction pattern analysis were both carried out by the Gatan Digital Micrograph software.[34]

Synthesis of Coordination Complexes

Synthesis of [Ca(μ-C₉H₈O₈)(H₂O)₄]ₙ, (CPTCA-Ca). Crystals were grown from evaporation of an aqueous solution of *cis,cis,cis,cis*-1,2,3,4-cyclopentanetetracarboxylic acid (0.4920 g, 0.2 mol L^{-1}) and $Ca(OH)_2$ (0.1126 g, 0.2 mol L^{-1}) at room temperature. Colorless plates suitable for X-ray analysis grew within three weeks.

Analysis calc. for [Ca(μ-$C_9H_8O_8$)(H_2O)$_4$]$_n$: C, 30.34%; H, 4.53%. Found: C, 30.28%, H, 4.40%. Water loss in TGA calculated for CPTCA-Ca: 20.21% for four water molecules. Found: 21.55%. IR (cm^{-1}): 3583 (w), 3313 (w, b), 2976 (w), 2721 (w), 2479 (w), 1981 (w), 1698 (m), 1512 (s), 1427 (s), 1334 (m), 1312 (m), 1258 (m), 1225 (m), 1208 (m), 1152 (w), 1103 (w), 1090 (w), 1051 (w), 1027 (w), 1010 (w), 941 (w), 911 (w), 867 (w), 844 (w), 812 (w), 799 (w), 718 (w), 642 (w).

Crystal data for [Ca(μ-$C_9H_8O_8$)(H_2O)$_4$]$_n$: M = 356.30 g mol^{-1}, orthorhombic, space group *Abm2*, a = 5.6391(5) Å, b = 20.406(2) Å, c = 11.8487(11) Å, V = 1363.5(2) Å^3, Z = 4, μ = 0.526 mm^{-1}, D_c = 1.736 g cm^{-3}, F_{000} = 744.0, 8845 reflections collected, 1863 unique (R_{int} = 0.0622). Final GOF = 1.084, R_1 = 0.0442 (1689 reflections with $I \geq 2\sigma(I)$, wR_2 = 0.1063.

Synthesis of [Ca($C_{12}H_{11}O_6$)$_2$(H_2O)$_4$]·1.25H_2O, (CHHCA-Ca). Crystals were obtained at room temperature by layering a solution of all-*cis*-1,2,3,4,5,6-cyclohexanehexacarboxylic acid in butanol-1 (8 mL, 0.0108 mol L^{-1}) on to an aqueous solution of $Ca(OH)_2$ (4 mL, 0.0233 mol L^{-1}). Insufficient sample was obtained for analysis other than single crystal X-ray crystallography.

Crystal data for [Ca($C_{12}H_{11}O_6$)$_2$(H_2O)$_4$]·1.25H_2O: M = 828.07 g mol^{-1}, monoclinic, space group *C2/c*, a = 22.632(5) Å, b = 10.473(2) Å, c = 29.189(6) Å, β = 105.622(2)°, V = 6663(2) Å^3, Z = 8, μ = 0.282 mm^{-1}, D_c = 1.651 g cm^{-3}, F_{000} = 3436.0, T = 100 K, 39546 reflections collected, 9657 unique (R_{int} = 0.0403). Final GOF = 1.131, R_1 = 0.0666 (7394 reflections with $I \geq 2\sigma(I)$), wR_2 = 0.2142.

Single-Crystal Structure Determination

Crystallographic data for CPTCA-Ca and CHHCA-Ca have been deposited with the Cambridge Crystallographic Data Centre (deposition numbers 1578272 and 1578273). The X-ray single crystal data for CPTCA-Ca were collected at 120.0(2) K on an Agilent XCalibur (Sapphire-3 CCD detector, graphite monochromator) 4-circle kappa diffractometer using graphite monochromated MoKα radiation (λ = 0.71073 Å). The data for the weakly diffracting crystals of CHHCA-Ca were collected at 100.0(2) K on a Rigaku Saturn 724+ diffractometer at station I19 of the Diamond Light Source synchrotron (undulator, λ = 0.6889 Å, ω-scan, 1.0°/frame) and processed using the Bruker APEXII software.[35] Both structures were solved by direct methods and refined by full-matrix least squares on F^2 for all data using Olex2[36] and SHELXTL[37] software. All non-disordered, non-hydrogen atoms were refined in an anisotropic approximation. The hydrogen atoms were placed in calculated positions and refined in riding mode. The structure CHHCA-Ca also contains some severely disordered solvent molecules (32 electrons) that could not be properly modelled and their contribution to the structural factors was taken into account by applying MASK procedure of the Olex2 program package. The structures were visualized using X-Seed[38] and the molecular graphics were produced using POV-Ray.[39]

Microanalysis was performed by London Metropolitan University using a Thermo Scientific (Carlo Erba) Flash 2000 Elemental Analyser. Thermogravimetric analysis (TGA) was carried out using a Perkin Elmer Pyris 1 TGA coupled with a 500 amu Hiden mass spectrometer (MS), which allows the analysis of the volatiles generated by the thermal degradation of materials. The volatiles monitored by the MS are CO, CO_2, and H_2O. Thermal analysis was carried out from 20 ºC to 500 ºC at a rate of 10 ºC/min. See Figure S14 and Figure S15 in the Supporting Information for the PXRD pattern and the TGA thermogram for CPTCA-Ca, respectively.

Results and Discussion

Construction and Validation of a Model Dishwasher Test System

Two model set-ups (Figure 3) have been constructed to mimic the main wash cycle of the real-life dishwasher. For a detailed dishwasher procedure and the dishwasher detergent formula see the Supporting Information. The model set-ups in Figure 3a & 3b were used to explore the growth of calcium carbonate under different chemical conditions. Two variants of the model system were explored with and without a circulating peristaltic pump which was designed to mimic the continual flow of dishwasher medium onto the substrate. While the phases of calcium carbonate can be affected and controlled by different shear rates,[40] in the present case agitation in this way did not result in any significant differences in the nature of deposits formed and their distribution on the target substrates (see Supporting Information). As a result, the simpler, non-circulating geometry shown in Figure 3a was used throughout the work.
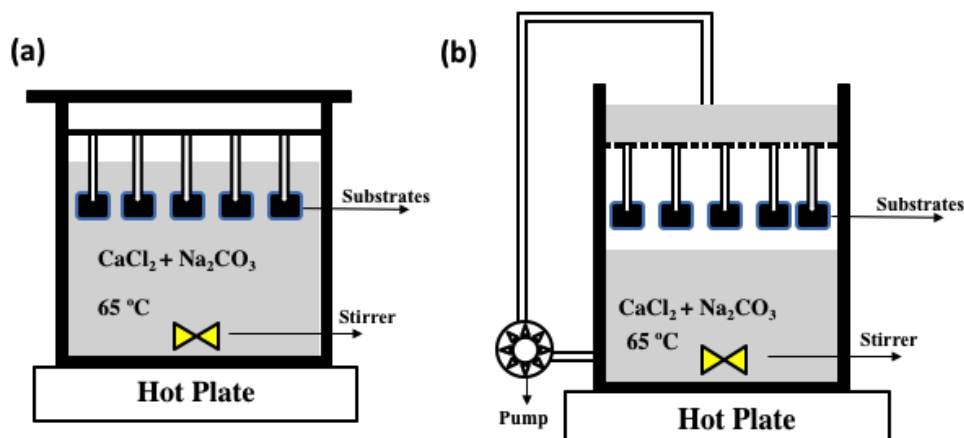
Figure 3. The model setting with the absence of a pump (a) and with the presence of a pump (b). Experimental conditions: $T = 65\ ^{\circ}C$, pH = 10.5, stirring rate = 100 rpm, $SI_{(aragonite)} = 2.78$, $SI_{(calcite)} = 3.72$, [Ca] = 2.75 mmol L^{-1}, [Mg] = 0.86 mmol L^{-1}, [CO$_3$] = 18.00 mmol L^{-1}. (See Equation S1 and Equation S2 in the Supporting Information for the calculation of saturation index (SI) for aragonite and calcite, respectively).

Table 2 lists the detailed differences between the model and real dishwasher systems. The difference mainly lies in two aspects: the presence of the pumping system and the simplified

cycle procedure in the model system. The exclusion of the pumping system in the model system removes the shear effects and agitation effects caused by the spraying action. The model system also excludes the prewash cycle, reduces the time for both cold rinse and hot rinse, and drying is simply in the air at room temperature (RT) rather than at high temperature up to 60 ºC. Deionized (DI) water was used in the rinsing cycle to clean substrates after crystallization so as to ensure that the crystals observed on surfaces arose from deposition from the washing solution in the main wash cycle rather than residues from hard water in the rinsing cycle. For the experimental details for the full-scale dishwasher and the model system, see the Supporting Information and Experimental Section, respectively.
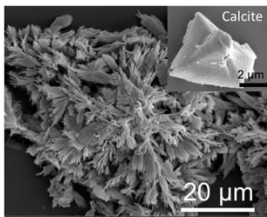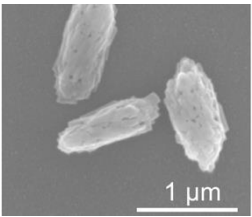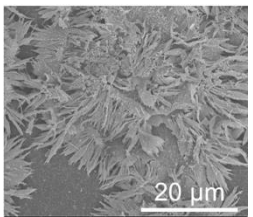
Table 2. Comparison of the full-scale dishwasher and the model system.

Procedure	Model system (no pump)	Dishwasher
Pre-wash	no pre-wash	pre-wash for 9 min (when present)
Main wash	60 min (500 mL)	36 min (5.0 L)
Stirring	100 rpm	pumping and spraying systems
T_{max}	65 °C	ramp up from cold to 65 °C
Cold rinse	1 min with DI water at RT	4 min (water with Ca^{2+}, Mg^{2+} at RT)
Hot rinse	1 min with DI water at 60 °C	21 min (water with Ca^{2+}, Mg^{2+} up to 60 °C)
Drying	RT	30 min at 40-60 °C

Two sets of validation samples were produced from the dishwasher and model system using an inhibitor-free detergent (the nil-HEDP formula, see Experimental Section). Polymethylmethacrylate (PMMA) sheets and glass sheets were used as substrates in the model system, while PMMA slides and glass tumblers were used as substrates for the dishwasher. Deposition of calcium carbonate on glass and PMMA substrates was examined by immersing them in a calcium and magnesium chloride solution (simulated hard water) in the presence of the

nil-HEDP detergent formula simulant at 65 ºC of 60 min. The samples then were rinsed and dried. Each procedure was repeated five times so as to obtain enough deposits for PXRD analysis. The clarity of the dishwasher samples was graded via a camera analysis rating system (0%-100%, see Experimental Section) and samples from the model system was by naked eye evaluation, with 100% clarity indicating no film on surfaces. Both sets of samples were analyzed by PXRD, FTIR, SEM, and TEM and the characterization results are summarized in Table 3.

Table 3. The deposits observed from the model system and a real dishwasher on the PMMA and the glass substrates with the nil-HEDP formula after five repeated cycles.

	Model system		Dishwasher	
	Glass	PMMA	Glass	PMMA
Clarity	40%	10%	75.2%	15.5%
Optical image				
PXRD	Calcite	Calcite = 1% (± 3%); Aragonite(001) = 99% (± 3%)	Insufficient sample	Calcite = 1% (± 3%); Aragonite(001) = 99% (± 3%)
SEM				

Without the inhibitory effects of the HEDP, the surface deposition of calcium carbonate, particularly on plastic was obvious, and after five repeated cycles, PMMA slides were heavily scaled. On the basis of the PXRD analysis (Figure S9) and SEM images (Table 3), the morphologies and the polymorphic forms of the calcium carbonate crystals from the real dishwasher were well-replicated by the model system. It is also interesting to observe that

different polymorphs have a different preference towards different substrates. The PXRD data indicates that flower-like aragonite with (001) preferred orientation along with trace calcite was observed on the PMMA substrate in both real and model systems, while rice-like calcite crystals were seen for the glass samples. Such large aragonite crystals observed on PMMA with preferred orientation have not been previously reported. The detailed SEM images and the confirmation of the preferred orientation of the aragonite (001) via TEM are shown in Figure S8 and Figure S10, respectively. The corresponding FTIR spectra for deposits identification is shown in Figure S7 in the Supporting Information.

Inhibition Performance Screening

The inhibition efficiency of the candidate inhibitors was evaluated in the presence of simulated hard water and a simulated detergent mixture (the nil-HEDP formula) in the model system. HEDP with its high inhibition efficiency and consequent retention of 'shine' for any substrate under dishwasher conditions, serves as a benchmark inhibitor. Deposition of calcium carbonate on glass and PMMA substrates at 65 $^{\circ}$C in simulated hard water in the presence of the nil-HEDP detergent formula for five cycles of 60 min each, acts as a control experiment for the inhibition performance of the candidate inhibitors.
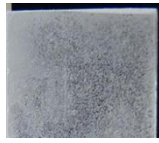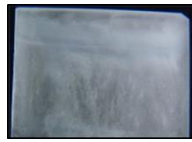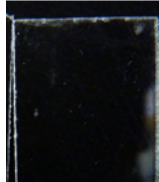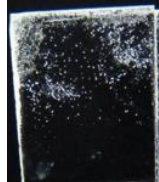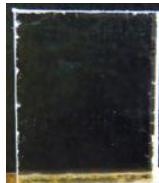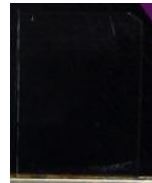
A series of commercially available cyclic polycarboxylic acids with 5-, 6-, 10- and 12-membered rings and with two or more carboxylic acid groups were evaluated as candidate inhibitors (Figure 2). A further phosphorus-containing compound phytic acid (PA – a saturated cyclic acid that can be found in cereals and grains[41]) was also evaluated for comparison. The inhibition performance of the selected inhibitors, except CHTTCA, was evaluated at the same concentration as HEDP (0.112 mmol L^{-1}). CHTTCA is a mixture of *cis-* and *trans-* isomers, hence double the amount was applied (see Table S3 in the Supporting Information).

The inhibition performance of the candidate inhibitors can be simply evaluated by visual inspection. Typically, for most of the inhibitors tested, film formation was observed after two or three cycles. Candidate inhibitors that were capable of retaining shine as efficiently as HEDP after five repeated cycles, were deemed to be effective inhibitors. Some candidate inhibitors that exhibited some inhibition ability in the first cycle, with film formation occurring in subsequent cycles, were also deemed ineffective. The screening outcomes of twenty-eight different candidate inhibitors including HEDP are given in Table 4.

Table 4. The inhibition performance screening results after three repeated cycles. The best-performing inhibitors (HEDP, PA and 1: 1 mixture of CPTCA and CHHCA) were run for five cycles. 'Pass' means that a fully shiny surface was retained, while 'fail' implies some observable film formation on the surface. A concentration of 0.112 mmol L^{-1} was used in all cases except the CHTTCA (0.224 mmol L^{-1}).

No.	Inhibitor	Glass	PMMA	No.	Inhibitor	Glass	PMMA
1	HEDP	pass	pass	16	PA	pass	pass
2	TMCPDA	fail	fail	17	GTA	fail	fail
3	CPDA	fail	fail	18	DHDAD	fail	fail
4	CPTCA	fail	pass	19	GA	fail	fail
5	THFTCA	fail	fail	20	PDA-12	fail	fail
6	FA	fail	fail	21	PDA-13	fail	fail
7	QA	fail	fail	22	SPS	fail	fail
8	CHDAA	fail	fail	23	BTCA	fail	fail
9	CHDA	fail	fail	24	BTTCA	fail	fail
10	CHTCA-135	fail	fail	25	BPCA	fail	fail
11	CHTCA-124	fail	fail	26	BHCA	fail	fail
12	TPCHTCA	fail	fail	27	DPA	fail	fail
13	CHTTCA	fail	fail	28	PZDA	fail	fail
14	CHHCA	pass	fail	29	GTDH	fail	fail
15	CPTCA + CHHCA	pass	pass	30	TTCDTCA	fail	fail

Table 5. Surface clarity with and without effective inhibitors.

Compositions	PMMA	Glass
nil-HEDP formula (No inhibitor)		
with HEDP		
with PA		
with CPTCA		
with CHHCA		
with CPTCA + CHHCA		

As can be seen from Table 5, when using the nil-HEDP formula (in the absence of any inhibitor), film formation on the surfaces of both substrates was immediately obvious. After the screening test, only HEDP and the other phosphorus-based inhibitor, PA, resulted in a complete inhibition of filming on both substrates after five repeated cycles in the model dishwasher system.

Even though PA is non-toxic,[42] as a phosphate-based compound, it has a negative impact on the environment (*i.e.* eutrophication) and hence cannot be regarded as an environmentally friendly alternative to HEDP. All the other carboxylate candidate inhibitors failed to prevent the formation of a film on the surface of at least one substrate after two or three repeated cycles. Interestingly, however, two carboxylic acid-based inhibitors gave a substrate-specific inhibition. CPTCA showed excellent inhibition of filming on PMMA without having a significant effect on glass, while CHHCA prevented filming on glass but proved ineffective on PMMA. As a result, the experiment was repeated using a mixture of these two compounds, each at 0.112 mmol L^{-1}. This resulted in inhibition of filming on both substrates and comparable performance to the phosphorus-based systems (Table 4 and Table 5). As a result, the two cyclic polycarboxylates, CPTCA and CHHCA in combination, represent a viable phosphate-free calcium carbonate inhibitor system.

The high-shine surfaces shown in Table 5 that were obtained in the presence of HEDP and a 1:1 mixture of CPTCA and CHHCH, were further examined by SEM (Figure 4). When produced in the presence of the effective inhibitor(s), all surfaces appeared to retain their shine to the naked eye but a few amorphous clusters were evident by SEM. This indicates that the presence of small amorphous cluster deposits does not affect visual 'shine' as none of the effective inhibitors eliminate amorphous clusters from surfaces. Therefore, for an inhibitor to be effective, it may need to, at least, stabilize the deposit as amorphous clusters and prevent them from further growth even after repeated cycles of deposition.
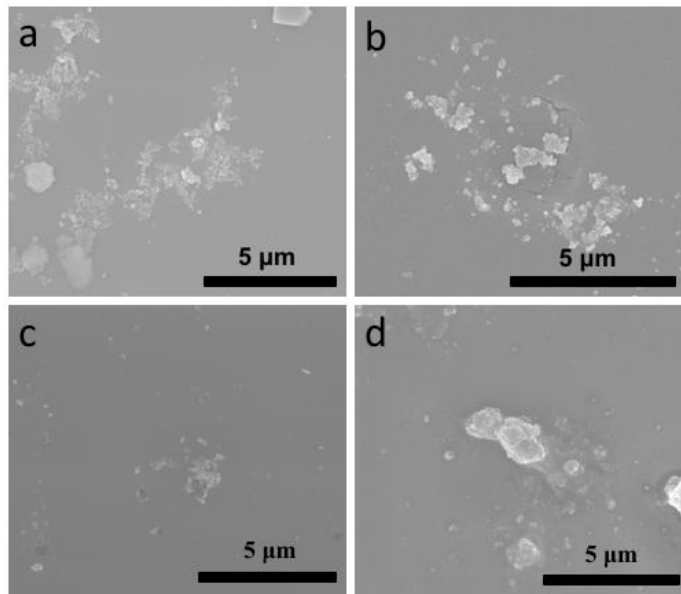
Figure 4. (a) and (b) deposits observed by SEM on a visually clear surface obtained using HEDP inhibitor on glass and PMMA, respectively; (c) and (d) deposites observed by SEM on glass and PMMA respectively using a 1 : 1 mixture of CPTCA and CHHCA.
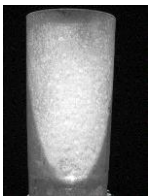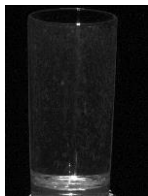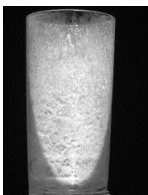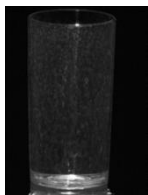
Performance in a Real Dishwasher

The best-performing inhibitors, namely a 1 : 1 mixture of CPTCA and CHHCA from the initial screening test, were further evaluated in a real dishwasher up to 30 cycles. The test materials used were glass and polystyrene tumblers.

The experimental procedure followed is a standard dishwasher procedure as described in Supporting Information. The Miele GSL R-zeit dishwasher model was used. A full washing process in the standard dishwasher procedure includes prewash, main wash, cold rinse, heated rinse and drying. In the main wash, 5 liters of fresh 'hard' water ([Ca] = 2.75 mmol L^{-1}; [Mg] = 0.86 mmol L^{-1}; [CO_3] = 18.00 mmol L^{-1}) were added and heated to 65 ºC. The alkaline detergent with the test inhibitor(s) was added at this stage. The main wash step lasted for 60 min, followed by rinse and drying cycles. This procedure was applied for 30 full wash cycles containing both glass and plastic substrates. The resulting surfaces of both the glass and the plastic (polystyrene)

samples either without inhibitor, with HEDP or with a 1 : 1 mixture of CPTCA and CHHCA, are presented in Table 6. The inhibition performance of a combination of CPTCA and CHHCA was determined again based on the clarity that the inhibitors can retain in comparison to the HEDP standard. The test results obtained were in line with the performance observed using the model system, which confirms the inhibition effectiveness of the combined CPTCA and CHHCA. Hence, the new inhibitors in combination can retain the shine as efficiently as HEDP.

Table 6. Evaluation of the new inhibitors under real dishwasher conditions.

Substrate	Cycles	No inhibitor	with HEDP	with CPTCA & CHHCA
		–	0.112 (mmol L^{-1})	0.112 + 0.112 (mmol L^{-1})
Glass	Cycle 15			
	Cycle 30			
Plastic	Cycle 15			
	Cycle 30			

At the end of cycle 30, even though the samples were visually clear to the naked eye, some spots can still be captured by the camera system from surfaces of the plastic samples obtained

both by the presence of HEDP and a mixture of CPTCA and CHHCA. These spots may arise from two possible sources: The ineffectiveness of the inhibitors to stop the build-up of spots once they form on the surface (see Figure 4 and the corresponding discussion) or as a result of the drying of hard water left on surfaces during the drying cycle. Therefore, further strategies are still needed for complete prevention of spots formation in the full system on repeated washing.

Understanding Selective Inhibition

To understand this inhibition substrate specificity of CPTCA and CHHCA, the glass and PMMA sheets that exposed to CPTCA and CHHCA separately were further examined using PXRD and SEM. The characterization results are given in Table 7.
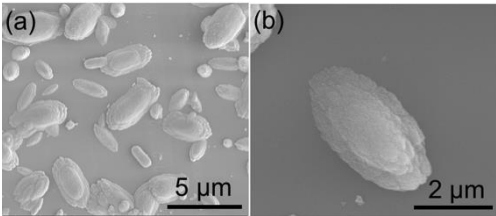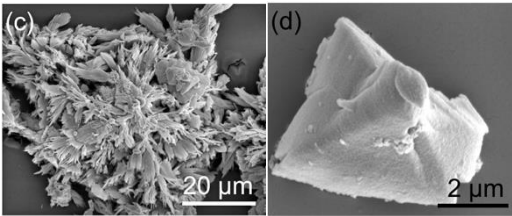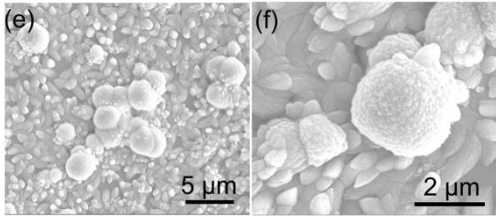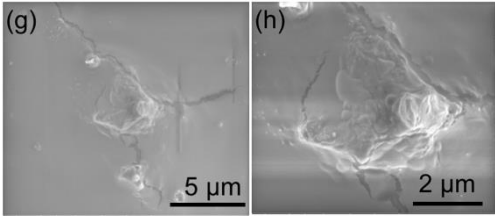
When using the nil-HEDP formula, both PMMA and glass substrates exhibit significant filming. The PMMA sheets exhibited both flower-like aragonite (001) (Table 7c) and small amounts of pyramid-like calcite (Table 7d), while rice-like calcite was observed on the glass substrate (Table 7a & b). Comparison of samples produced using the nil-HEDP formula with those treated with CPTCA shows that the surface appearance changed after adding CPTCA after three repeated cycles 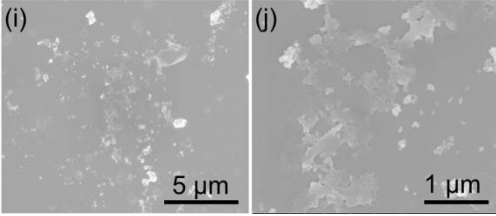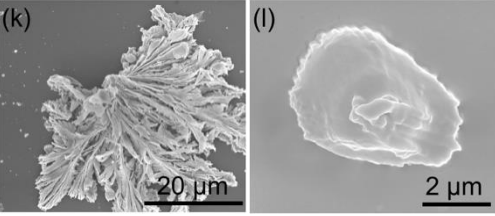for the PMMA substrate but not for glass. The flower-like aragonite deposits on the PMMA sheets were completely inhibited, and the growth of pyramid-like calcite was also suppressed although small pyramid-like calcite crystals, which typically formed in the first cycle, can still be observed on the PMMA (Table 7g & h). This is consistent with the observation by Reddy[12] that CPTCA is an excellent inhibitor for seeded calcite in solution. CPTCA is also an excellent inhibitor for seeded calcite grown on a surface. However, CPTCA is ineffective at inhibiting the growth of calcite on glass (Table 7e & f). The calcite crystals formed on glass in the presence of CPTCA are similar in amount and morphology to those observed in

samples produced without inhibitor (Table 7a & b). The PXRD data confirms that the crystals on glass are calcite (see Figure S11 in Supporting Information).

CHHCA, on the other hand, has a similar inhibition effect but is opposite to that of CPTCA. The SEM images show that the aragonite (001) and calcite crystals observed on the PMMA sheet (Table 7k & l) are similar to those found on inhibitor-free samples (Table 7c & d). This is confirmed by the PXRD pattern shown in Figure S12 in Supporting Information. This means that CHHCA has no significant effect in inhibiting the crystal growth on the PMMA substrate. However, the inhibitory effectiveness of CHHCA on the glass slide is obvious, with only a tiny amount of amorphous deposits observed (Table 7i & j).

It seems reasonable to question why the substrate-specific inhibition observed for CHHCA and CPTCA does not occur for the phosphate-containing inhibitors PA and HEDP, both of which retain surface shine regardless of the substrate. Possible explanations include better synergistic effects between the phosphate-containing inhibitors and the polymer or the intrinsic advantage of the phosphate functional groups. Studies of crystallization of calcium carbonate on self-assembled monolayers (SAMs) have demonstrated the intrinsic advantage of the phosphate functional groups. It shows that some functional groups ($-OH$, $-COO^-$ and $-SO_3^{2-}$) can only orientate one specific face of calcite, while $-PO_3^{2-}$ is capable of inducing a series of calcite faces.[43] Further studies are still required to understand the other factors, such as surface properties of PMMA and glass and the underlying interactions among substrate, minerals, and additives.

Table 7. The PMMA and glass sheets produced in the model system with the nil-HEDP formula, CPTCA and CHHCA.

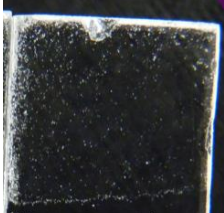|	Glass	PMMA
nil-HEDP formula (no inhibitor)		
Optical image		
PXRD	Calcite	Calcite = 1% (± 3%); Aragonite(001) = 99% (± 3%)
SEM		
With CPTCA		
Optical image		
PXRD	Calcite	Insufficient sample
SEM		
With CHHCA		
Optical image		
PXRD	Insufficient sample	Aragonite(001) and calcite
SEM		
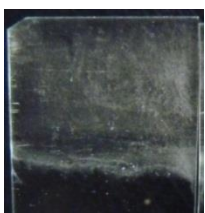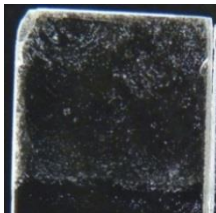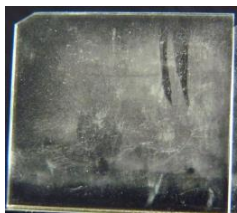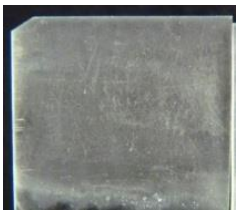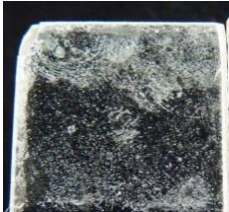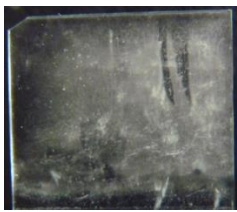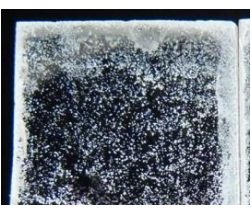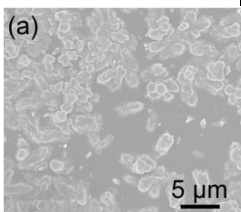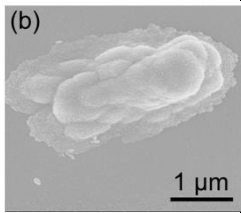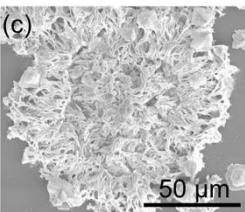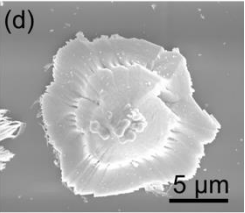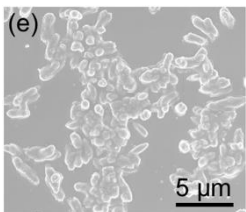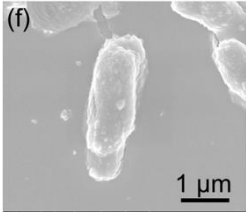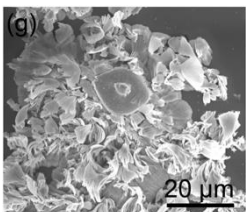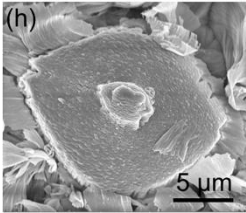
The Inhibition Mechanism of HEDP

A simple experiment was carried out to assess whether the HEDP inhibitor acts before nucleation or during crystal growth. Two sets of samples were prepared each involving two glass slides and two PMMA slides. In the first cycle for both experimental sets (A) and (B), the nil-HEDP formula was added. After crystallization for 60 min, the samples were rinsed with DI water and left to dry in air. One glass sheet and one PMMA sheet from each experimental set were retained for further analysis by SEM and PXRD while the other substrates from the first cycle were replaced in the crystallization apparatus with new solutions and continued to crystallization in the second cycle. In the second cycle, Set A involved the standard nil-HEDP formula, while the full HEDP formula was added to Set B. The resulting surfaces and corresponding characterization are shown in Table 8.

As can be seen from Table 8, with seed crystals from the first cycle preexisting on both surfaces, the presence of HEDP did not prevent further deposition on PMMA and crystals on the PMMA substrate grew as if there was no inhibitor. This is different from the observation made by Nancollas,[24] which suggested HEDP an effective inhibitor for seeded aragonite. In contrast, for glass samples, no further growth was observed in the presence of HEDP (Set B, after the second cycle). SEM and PXRD data indicate that HEDP was especially effective as an inhibitor for calcite grown on glass but had no obvious inhibition ability towards aragonite and calcite on the PMMA (The calcite was only observed on the top of the aragonite but not directly from the PMMA surface). However, as long as there were no preexisting crystals on the PMMA slides, HEDP was an effective inhibitor for both substrates. This indicates that an inhibitor may have different inhibition mechanism towards different polymorphs of the same mineral in different crystallization stages. For aragonite crystals, HEDP influenced the extent of their formation,

however, once they formed, HEDP did not exert further inhibition. For calcite crystals, on the other hand, HEDP was an effective inhibitor both before and after nucleation on glass.[44-45] This is probably why plastic, in particular, suffers more filming in the dishwasher than glass.

Table 8. The samples from Set A and Set B with the corresponding characterization from SEM and PXRD.

	Set A		Set B	
Description	No inhibitor for both cycles		No inhibitor @ 1st cycle and inhibitor @ 2nd cycle	
	Glass	PMMA	Glass	PMMA
The first cycle				
Clarity	30%	60%	30%	60%
The second cycle				
Clarity	0%	20%	30%	10%
SEM				
PXRD (Figure No.)	Calcite (Figure S13)	Aragonite (001) and calcite (Figure S13)	Calcite (Figure S13)	Aragonite(001) and calcite (Figure S13)

Structural Characteristics of an Efficient Inhibitor

Phosphonate inhibitors have been used in mineral inhibition since they were first patented in 1863[46] and cyclic polycarboxylic acids were not of interest until the environmental drawbacks of phosphonates were realized. The effectiveness of phosphonate-containing inhibitors is likely to be rooted in the high polarity of the phosphate functional group and hence, to make up for the deficiency in polarity, more carboxylates in a more structurally preorganized fashion are needed to exhibit effective interactions to the calcium ions of the nucleating crystal or growth region.
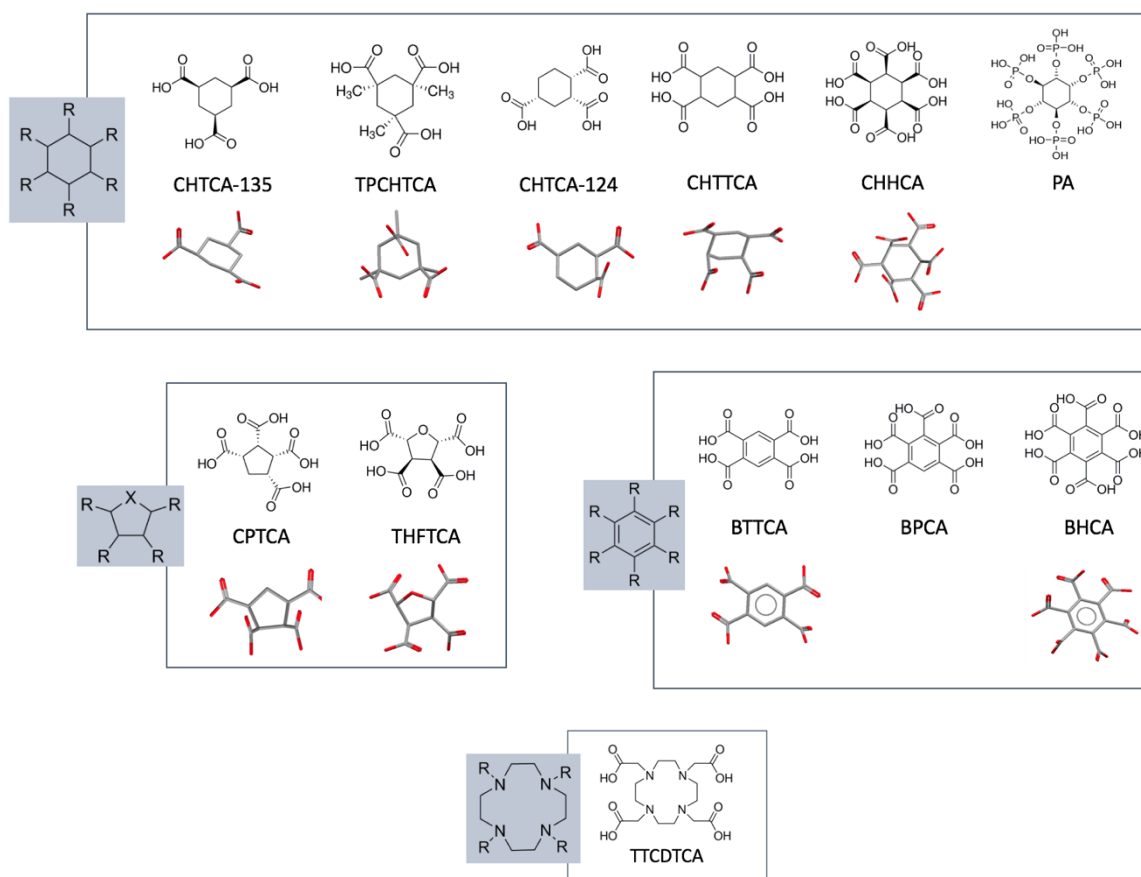
Figure 5. Candidate inhibitors with three or more carboxylate groups arranged according to their backbone structures (R = COOH, PO$_3$H or H; X = C or O). The corresponding X-ray crystallographic structures obtained from the Cambridge Structure Database (CSD) are shown where available highlighting functional group spatial arrangement. Reference codes for CSD structures: CHTCA-135 (BANGON),[47] TPCHTCA(DEVCOW);[48] CHTCA-124 (EZOPIU),[49] CHTTCA (EJEQOZ);[50] CHHCA (GOHWAD);[51] CPTCA (AWUVEU);[52] THFTCA (ZEZLEV);[53] BTTCA (PYMELL12);[54] BHCA (MELLIT);[55]

It has been suggested that diphosphonate functional groups that simultaneously access surface binding sites are sufficient for mineral inhibition.[56] In the case of the carboxylate-containing inhibitors, this simple relationship does not hold. Amjad[14] observed that benzene-1,2,3,4,5,6-hexacarboxylic acid has the best inhibition performance for seeded calcite, followed by isophthalic acid (benzene-1,3-dicarboxylic acid), indicating that dicarboxylic acid groups exert poorer inhibition effects. From the inhibition screening results in this project, none of the candidates with two carboxylate groups work as an efficient inhibitor. Amjad[57-58] and Reddy[12] suggested that cyclic poly(carboxylate) acids are required to have four or six carboxylate groups that attach to different carbon atoms in the ring to be sufficiently effective for seeded calcite. These workers did not study inhibition ability towards aragonite, however, the effectiveness of the inhibitors CPTCA and CHHCA do support this requirement regarding the number of functional groups. However, under dishwasher conditions, not all of the carboxylic acids with four or more carboxylate group are effective inhibitors (Figure 5). For example, neither benzene-based polycarboxylic acids (BTTCA, BPCA & BHCA) nor the saturated ring based candidate inhibitors CHTTCA, THFTCA and TTCDTCA, which have a similar backbone to CPTCA and CHHCA, work as efficient inhibitors. For the benzene-based polycarboxylic acids (BHCA, Figure 5), the orientation of carboxylates attached is essentially planar due to the structure of the aromatic ring, and the simultaneous binding of all of the carboxylate groups to a growing crystal surface is not possible, indicating the importance of conformational freedom.[54] The requirements on the number and the orientation of attached functional groups and conformational freedom are well demonstrated by the inefficacy of tetrahydrofuran-2c,3t,4t,5c-tetracarboxylic acid (THFTCA) in contrast to the very closely related and very effective *cis,cis,cis,cis*-CPTCA. The conformational freedom is a balanced between flexibility and rigidity in the backbone. Molecular

flexibility allows multiple carboxylate groups to attach to emerging nucleus,[13] while molecular rigidity, as long as it results in suitable preorganization for interaction can reduce entropic effects.[59]
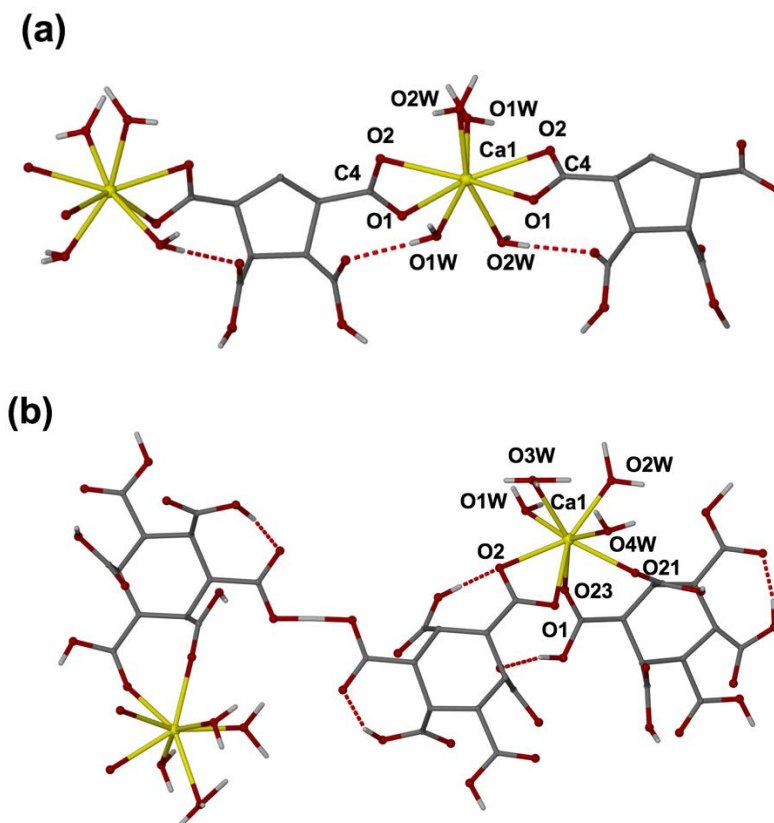
Figure 6. (a) The crystal structure of [Ca(μ-$C_9H_8O_8$)(H_2O)$_4$]$_n$ (CPTCA-Ca). Selected bond lengths (Å) for eightfold coordination: Ca(1)-O(1) = 2.533(2), Ca(1)-O(2) = 2.496(2), Ca(1)-O(1W) = 2.438(2), Ca(1)-O(2W) = 2.399(2). (b) The crystal structure of [Ca($C_{12}H_{11}O_6$)$_2$(H_2O)$_4$]·1.25H_2O (CHHCA-Ca). Selected bond lengths (Å) for eightfold coordination: Ca(1)-O(1) = 2.500(2), Ca(1)-O(2) = 2.4550(19), Ca(1)-O(21) = 2.373(2), Ca(1)-O(23) = 2.413(2), Ca(1)-O(1W) = 2.386(2), Ca(1)-O(2W) = 2.404(3), Ca(1)-O(3W) = 2.603(3), Ca(1)-O(4W) = 2.420(3). The hydrogen bond is omitted for clarity.

In order to further understand the calcium coordination mode of the successful inhibitors, crystalline calcium complexes of CPTCA and CHHCA were prepared by slow evaporation of calcium hydroxide solutions containing the oligo carboxylic acids. This resulted in the isolation of crystals of formula [Ca(μ-$C_9H_8O_8$)(H_2O)$_4$]$_n$ and [Ca($C_{12}H_{11}O_6$)$_2$(H_2O)$_4$]·1.25H_2O, denoted as CPTCA-Ca and CHHCA-Ca, respectively, which were characterized by single crystal X-ray crystallography. In CPTCA-Ca, the ligand is in its dianionic form while the ligands in

CHHCA-Ca are singly deprotonated. These single crystal structures were obtained at acidic pH and hence not under directly analogous conditions to the dishwasher environment. As a result, they may not be representative of the interaction between the inhibitor and calcium ions in a dishwasher at higher pH. However, the crystal structures may be relevant for understanding the possible structural features for an efficient inhibitor in terms of ligand binding mode and backbone conformational characteristics. Figure 6 shows the X-ray structures of CPTCA-Ca and CHHCA-Ca. While CPTCA binds only via four-membered chelate rings, CHHCA exhibits both four and seven-membered ring coordination. Even though both acids are the all-*cis* isomers, the carboxylate groups attached to the backbone have different conformations. For example, the carboxylic acids on the 1,4 position in CPTCA-Ca have a larger angle (154.9°) to the backbone compared to the 2,3 position (111.1°). For CHHCA-Ca, the angles between the two adjacent carboxylate groups to the backbone are also different. This conformational variety not just limited to CPTCA and CHHCA but can also be observed from the other crystallographically-derived ligand structures shown in Figure 5. The orientation distribution of carboxylic acids on CHHCA can be viewed as a combination of CHTCA-135 and TPCHTCA. It seems that it is either the lack of sufficient functional groups attached to the cyclohexane ring or the presence of two adjacent functional groups as in CHHCA that leads to the ineffectiveness of CHTCA-135 and TPCHTCA. The former explanation is perhaps more likely give the ineffectiveness of CHTCA-124 and CHTTCA, both of which have two adjacent functional groups. Even though the structural data does not reveal any obvious structural or stereochemical correlation with inhibition performance, all the subtle differences in structure should be examined carefully. It is those subtle differences that can lead to substantial difference in inhibition performance.[5, 54, 58]

Although it is still unknown specifically how the inhibitor interacts with the growing nucleus or crystal, it is clear that, for a nucleus/particle to grow, the solute particles need to interact with one another and hence the effectiveness of an inhibitor may rely on its ability to weaken or disrupt this solute aggregation[61] or molecular recognition at the interface[56, 59, 62-64] and hence change the energy required to form a new interface.[65] It has been suggested that the ability of an inhibitor to weaken or disrupt the solute aggregation is related to electrostatics as well as stereochemistry of an inhibitor.[66] From the inhibitor structures tested, it seems that effective binding is related to the number and the orientation of functional group as well as the conformational freedom of the backbone structure. Volkmer *et al*.[67-68] and Didymus[69] have further related the inhibition of crystallization to critical charge density. It is observed that the crystallization of calcium carbonate switches from stabilization of less stable polymorphs to inhibition of crystallization when above a critical charge density in terms of the number of carboxylate residues per unit area. This is probably why the benzene-based polycarboxylic acids have limited conformation freedom but still are capable of inhibiting the seeded calcite as suggested by Richmond.[13] The charge density of small molecules, looking at the inhibitor molecule as a whole, should be related the polarity of a single functional group, the number of the functional groups and the size of the backbone. The magnitude of the overall negative charge density is determined by the type and number of the functional groups. This is probably why the phosphate-containing inhibitors with a higher polarity tend to be superior to those of carboxylate-based additives. The nature and size of backbone affect the magnitude of the overall negative charge and orientation of the functional groups, which together determine the charge distribution and its density. Current research focusing on the relationship between the critical charge density and inhibition efficiency of the known inhibitors is still rare. It may be

worthwhile to develop an accurate way to express the charge density of a molecule, hence its inherent properties can be related to its potential inhibition effectiveness toward specific crystals. The stereochemistry of the carboxylic acid distribution on the backbone should also be taken into consideration.

Conclusion

Crystallization experiments in a model system that effectively mimics real dishwasher scale deposits demonstrate that a combination of CPTCA and CHHCA show a similar inhibition performance to HEDP under dishwasher conditions and hence can form a potential environmentally friendly HEDP replacements. PA is also an effective inhibitor but as a phosphate-based compound, it is likely to have a negative impact on the environment. Interestingly, CPTCA and CHHCA are highly substrate specific as well as polymorph specific with CPTCA inhibiting aragonite growth on PMMA while CHHCA inhibits calcite growth on glass. The effectiveness of this cyclic carboxylic acid combination was further confirmed in a commercial dishwasher where shine was retained over 30 dishwasher cycles. While the carboxylate-containing inhibitors are not as effective as phosphate-containing inhibitors under dishwasher conditions at the same concentration by mass, combining the two carboxylate-containing inhibitors results in a similar inhibition performance to HEDP.

HEDP seems to have different inhibition mechanisms before and after nucleation. Without preexisting crystals on the surface, HEDP exerts powerful scale inhibition properties towards both glass and PMMA substrates. With seeded crystals on the surface, HEDP enables the retention of surface clarity by preventing calcite crystals from further growth on glass, but not on a PMMA substrate, where aragonite and calcite crystals grow as if there is no HEDP present. This observation indicates that HEDP has different inhibition behavior towards different

polymorphs once they grow: HEDP is effective inhibitor toward calcite both before and after nucleation, while for aragonite, it only exerts its inhibition ability before nucleation. It is, therefore, reasonable to suggest that if inhibitors have a different inhibition behavior[21, 69] and inhibition effectiveness[70] before and after nucleation, then they may have different structural impacts at nucleation and growth stages. Only when an inhibitor satisfies the requirements for both stages can it acts as an effective inhibitor under dishwasher conditions.

Under dishwasher conditions, cyclic polycarboxylic acids seem to need to reach a critical charge density to achieve a satisfactory inhibition performance. However, whether critical charge density is essential before the nucleation stage, during crystal growth or both requires further exploration. Nevertheless, in our case, cyclic polycarboxylic acids should have at least four all-cis functional groups attached to different carbon atoms in a relatively flexible cyclic backbone to work as an efficient inhibitor. CPTCA and CHHCA with their inhibition specificity, represent a good model for further research upon the inhibition behavior in different stages of crystallization and may find immediate practical application as phosphate-free real-world inhibitors.

Associated Content

Supporting Information

Dishwasher procedure including the dishwasher detergent formula, the comparison of the model set-ups with and without a circulating pump, and the validation of the model set-up to the real-life dishwasher are included in the Supporting Information. The purity and manufacturer of the compositions of the dishwasher formula are as shown in Table S2. The full name and quantity of the selected candidate inhibitors are shown in Table S3. This material is available free of charge

via the Internet at http://pubs.acs.org/. Crystallographic data in CIF format is available from the Cambridge Crystallographic Data Centre as deposition numbers 1578272 and 1578273.

Author Information

Corresponding Author

*E-mail: jon.steed@durham.ac.uk; Tel.: +44 191 334 2085.

Notes
The authors declare no competing financial interest.

Acknowledgements

References

(1) MacAdam, J.; Parsons, S. A., *Reviews in Environmental Science & Bio/Technology* **2004**, *3*, 159.
(2) Verch, A.; Gebauer, D.; Antonietti, M.; Cölfen, H., *Phys. Chem. Chem. Phys.* **2011**, *13*, 16811.
(3) Gomelya, N.; Hrabitchenko, V.; Trohimennko, A.; Shablij, T. J., *J. Enterp. Technol.* **2016**, *4*, (10(82)), 4-9.
(4) GI-XRD analysis of glass slides washed for 8 cycles in city spiked water. Procter & Gamble: Newcastle, 2010.
(5) Mann, S., *Biomineralization : Principles and concepts in bioinorganic materials chemistry*. Oxford University Press: Oxford, 2001; pp 38 -76.
(6) Koutsoukos, P. G., Calcium carbonate scale control in industrial water systems. In *The Science and Technology of Industrial Water Treatment*, Amjad, Z., Ed. CRC Press: Boca Raton, Florida, 2010; pp 39-60.

(7) Polyphosphate and silicate scale inhibitor for laundry and automatic dishwashing detergents. Rohm and Haas: 2006.

(8) Najibi, S. H.; Muller-Steinhagen, H.; Jamialahmadi, M., *J. Heat Transfer* **1997**, *119*, 767.

(9) Vetter, O. J.; Farone, W. A. In *Calcium carbonate scale in oilfield operations*, SPE Annual Technical Conference and Exhibition, Dallas, Texas, 27-30 September; Society of Petroleum Engineers: Richardson, TX, U.S.A: 1987; pp 307-322.

(10) Sand, K. K.; Rodriguez-Blanco, J. D.; Makovicky, E.; Benning, L. G.; Stipp, S. L. S., *Cryst. Growth Des.* **2012**, *12*, 842.

(11) Mann, S.; Didymus, J. M.; Sanderson, N. P.; Heywood, B. R., *J. Chem. Soc., Faraday Trans.* **1990**, *86*, 1873.

(12) Reddy, M. M.; Hoch, A. R., *J. Colloid Interface Sci.* **2001**, *235*, 365.

(13) Reddy, M. M.; Leenheer, J., *Ann. Environ. Sci.* **2011**, *5*, 41.

(14) Freeman, S. R.; Jones, F.; Ogden, M. I.; Oliviera, A.; Richmond, W. R., *Cryst. Growth Des.* **2006**, *6*, 2579.

(15) Dove, P. M.; Hochella Jr, M. F., *Geochim. Cosmochim. Acta* **1993**, *57*, 705.

(16) Berner, R. A.; Westrich, J. T.; Graber, R.; Smith, J.; Martens, C. S., *J. Am. Sci.* **1978**, *278*, 816.

(17) Hennessy, A. J.; Neville, A.; Roberts, K. J., *J. Cryst. Growth* **1999**, *198*, 830.

(18) Myerson, A. S.; Jang, S. M., *J. Cryst. Growth* **1995**, *156*, 459.

(19) Chen, T.; Neville, A.; Sorbie, K.; Zhong, Z., *Chem. Eng. Sci.* **2009**, *64*, 912.

(20) Xu, A. W.; Yu, Q.; Dong, W. F.; Antonietti, M.; Cölfen, H., *Adv. Mater.* **2005**, *17*, 2217.

(21) Anwar, J.; Boateng, P. K.; Tamaki, R.; Odedra, S., *Angew. Chem. Int. Ed.* **2009**, *48*, 1596.

(22) Ukrainczyk, M.; Stelling, J.; Vucak, M.; Neumann, T., *J. Cryst. Growth* **2013**, *369*, 21.

(23) Britt, D. W.; Hlady, V., *Langmuir* **1997**, *13*, 1873.

(24) Nancollas, G. H.; Sawada, K., *J. Pet. Technol.* **1982**, *34*, 645.

(25) Williams, G.; Sallis, J. D., *Calcif. Tissue Int.* **1982**, *34*, 169.

(26) Uchtman, V. A.; Gloss, R. A., *J. Phys. Chem.* **1972**, *76*, 1298.

(27) Uchtman, V. A., *J. Phys. Chem.* **1972**, *76*, 1304.

(28) Nygren, M. A.; Gay, D. H.; Catlow, C. R. A.; Wilson, M. P.; Rohl, A. L., *J. Chem. Soc. Faraday Trans.* **1998**, *94*, 3685.

(29) Sarig, S.; Kahana, F.; Leshem, R., *Desalination* **1975**, *17*, 215.

(30) Vetter, O. J., *J. Pet. Technol.* **1972**, *24*, 997.

(31) Ltd, B. A., TOPAS Academic: General profile and structure analysis software for powder diffraction data. In *Topas V2.0: General profile and structure analysis software for powder diffraction data*, Bruker AXS: Karlsruhe, 2000.

(32) *KnowItAll academic edition*, 2005; Bio-Rad Laboratories: 2005.

(33) *Scanning electron microscope*, Durham University, https://www.dur.ac.uk/electron.microscopy/facilities/fib/: 2016.

(34) *Digital Micrograph^{TM}*, 3; Gatan: Pleasanton, CA, 2007.

(35) Bruker, A. V., *Inc., Madison, WI, USA* **2009**.

(36) Dolomanov, O. V.; Bourhis, L. J.; Gildea, R. J.; Howard, J. A.; Puschmann, H., *J. Appl. Crystallogr.* **2009**, *42*, 339.

(37) Sheldrick, G. M., *Acta Crystallogr. Sect. A: Found. Crystallogr.* **1990**, *46*, 467.

(38) Barbour, L. J., X-Seed: A program for the manipulation and display of crystallographic models. Columbia, MO, USA, 1999.

(39) POV-Ray. Persistence of Vision Raytracer Pty.: 2012.

(40) Boulos, R. A.; Zhang, F.; Tjandra, E. S.; Martin, A. D.; Spagnoli, D.; Raston, C. L., *Sci. Rep.* **2014**, *4*, 3616.

(41) Lopez, H. W.; Leenhardt, F.; Coudray, C.; Remesy, C., *Int. J. Food Sci. Technol.* **2002**, *37*, 727.

(42) Grases, F.; Perelló, J.; Isern, B.; Costa-Bauzá, A., *Water SA* **2007**, *33*, 749.

(43) Aizenberg, J.; Black, A. J.; Whitesides, G. H., *J. Am. Chem. Soc.* **1999**, *121*, 4500.

(44) Jing, X., *Acta Phys. Sin. (Chinese Ed.)* **2006**, *55*, 1112.

(45) Amjad, Z.; Zuhl, R. W., Kinetic and morphological investigation on the precipitation of calcium carbonate in the presence of inhibitors. In *1996 NACE International Annual Conference and Exposition "Corrosion 2006",*, NACE International: Houston, Texas, United States, 2006.

(46) Gill, J. S., Development of scale inhibitors. In *NACE Corrosion Conference*, NACE International: Houston, United States, 1996.

(47) Bhogala, B. R.; Vishweshwar, P.; Nangia, A., *Cryst. Growth Des.* **2002**, *2*, 325.

(48) Rebek, J.; Marshall, L.; Wolak, R.; Parris, K.; Killoran, M.; Askew, B.; Nemeth, D.; Islam, N., *J. Am. Chem. Soc.* **1985**, *107*, 7476.

(49) Kaduk, J. A.; Allison F. M., **2016**, CCDC 1519525: Experimental Crystal Structure Determination, Cambridge Crystallographic Data Centre, DOI: 10.5517/ccdc.csd.cc1n05ys.

(50) Uchida, A.; Hasegawa, M.; Manami, H., *Acta Crystallogr. Sect. E* **2003**, *59*, 435.

(51) Thuery, P., Cyclohexane-1,2,3,4,5,6-hexacarboxylic acid tetrahydrate. CSD Private Communication, **2012**.

(52) Lin, J.-L.; Guo, X.-X.; Huang, W.-X., *Acta Crystallogr. Sect. E* **2011**, *67*, 1945.

(53) Feil-Jenkins, J. F.; Nash, K. L.; Rogers, R. D., *Inorg. Chim. Acta* **1995**, *236*, 67.

(54) Bo, Q. B; Zhao, S. Y.; Zhang, Z. W.; Sheng, Y. L.; Sun, Z. X.; Sun, G. X.; Chen, C. L.; Li, Y. X., **2014**, CCDC 608247: Experimental Crystal Structure Determination, Cambridge Crystallographic Data Centr. DOI: 10.5517/ccndxwt.

(55) Darlow, S., *Acta Crystallogr.* **1961**, *14*, 159.

(56) Davey, R.; Black, S.; Bromley, L.; Cottier, D.; Dobbs, B.; Rout, J., *Nature* **1991**, *353*, 549.

(57) Amjad, Z.; Pugh, J.; Reddy, M. M., Kinetic inhibition of calcium carbonate crystal growth in the presence of natural and synthetic organic inhibitors. In *Water Soluble Polymers*, Kluwer Academic Publishers: New York, 2002; pp 131-147.

(58) Amjad, Z., *Langmuir* **1987**, *3*, 224.

(59) Bromley, L. A.; Cottier, D.; Davey, R. J.; Dobbs, B.; Smith, S.; Heywood, B. R., *Langmuir* **1993**, *9*, 3594.

(60) Chung, J.; Granja, I.; Taylor, M. G.; Mpourmpakis, G.; Asplin, J. R.; Rimer, J. D., *Nature* **2016**, *536*, 446.

(61) Cheng, Y.; Yang, Z.; Tan, H.; Liu, R.; Chen, G.; Jia, Z., *Biophys. J.* **2002**, *83*, 2202.

(62) Black, S. N.; Bromley, L. A.; Cottier, D.; Davey, R. J.; Dobbs, B.; Rout, J. E., *J. Chem. Soc., Faraday Trans.* **1991**, *87*, 3409.

(63) Pradip; Rai, B.; Rao, T. K.; Krishnamurthy, S.; Vetrivel, R.; Mielczarski, J.; Cases, J. M., *Langmuir* **2002**, *18*, 932.

(64) Rohl, A.; Gay, D.; Davey, R.; Catlow, C., *J. Am. Chem. Soc.* **1996**, *118*, 642.

(65) Orme, C.; Noy, A.; Wierzbicki, A.; McBride, M., *Nature* **2001**, *411*, 775.

(66) Sommerdijk, N. A.; With, G. d., *Chem. Rev.* **2008**, *108*, 4499.

(67) Volkmer, D.; Fricke, M.; Agena, C.; Mattay, J., *J. Mater. Chem.* **2004**, *14*, 2249.

(68) Fricke, M.; Volkmer, D.; Krill, C. E.; Kellermann, M.; Hirsch, A., *Cryst. Growth Des.* **2006**, *6*, 1120.

(69) Didymus, J. M.; Oliver, P.; Mann, S.; DeVries, A. L.; Hauschka, P. V.; Westbroek, P., *J. Chem. Soc., Faraday Trans.* **1993**, *89*, 2891.
(70) Hennessy, A. J.; Neville, A.; Roberts, K. J., *J. Cryst. Growth* **1999**, *198–199, Part 1*, 830.

For Table of Contents Use

Phosphate-Free Inhibition of Calcium Carbonate Dishwasher Deposits

Yuexian Hong, Nathalie Letzelter, John S. O. Evans, Dmitry S. Yufit, Jonathan W. Steed*

In the unique high pH, high temperature environment of a dishwasher, inhibition of calcium carbonate deposition in the absence of environmentally unfriendly phosphate-based inhibitors remains a significant challenge. However, cyclopentane and cyclohexane based polycarboxylic acids prove to be effective highly substrate selective and polymorph specific inhibitors.